Electrochemical, Spectroscopic, and Spectroelectrochemical Properties of Synthetically Useful Supramolecular Light Absorbers with Mixed Polyazine Bridging Ligands

Eric Brauns, Sumner W. Jones, Jeff A. Clark, Sharon M. Molnar, Yuji Kawanishi,[†] and Karen J. Brewer*,[‡]

Department of Chemistry, Virginia Polytechnic Institute and State University, Blacksburg, Virginia 24061-0212

Received October 31, 1996[⊗]

The trimetallic complexes $[\{(bpy)_2M(dpp)\}_2Ru(dpq)]^{6+}$ (M = Ru^{II} or Os^{II}, bpy = 2,2′-bipyridine, dpp = 2,3-bis(2-pyridyl)pyrazine, and dpq = 2,3-bis(2-pyridyl)quinoxaline) have been prepared and the details of their spectroscopic, electrochemical, and spectroelectrochemical properties investigated. These mixed bridging ligand complexes are a new group of synthons that can be useful for the construction of supramolecular devices for a wide variety of functions. It is the presence of the terminal dpq ligand that allows for their incorporation into larger supramolecular systems. This dpq ligand serves as an acceptor ligand that will possess a lower lying π^* orbital than the dpp ligands once these chromophores are incorporated into larger systems. The $[\{(bpy)_2M(dpp)\}_2Ru(dpq)]^{6+}$ systems display overlapping terminal metal oxidations at 1.66 and 1.18 V vs Ag/AgCl for the Ru and Os systems, respectively. This indicates that within this framework, these terminal, M, metals are largely electronically uncoupled. No oxidative process for the central Ru metal center is observed within our solvent window. The $[\{(bpy)_2M(dpp)\}_2Ru(dpq)]^{6+}$ systems have M → dpp charge transfer (CT) lowest lying excited states. The $[\{(bpy)_2Ru(dpp)\}_2Ru(dpq)]^{6+}$ Ru → dpp CT state displays an emission centered at 775 nm with a lifetime of 65 ns at room temperature in deoxygenated CH_3CN solution. The details of the electrochemical, spectroscopic, and spectroelectrochemical studies of these supramolecular light absorbers and the dichloro synthons, $[\{(bpy)_2M(dpp)\}_2RuCl_2]^{4+}$, are reported herein.

Introduction

The light absorbing properties of $[Ru(bpy)_3]^{2+}$ have sparked interest in analog development aimed at preparing complexes that maintain the MLCT (metal to ligand charge transfer) excited state nature of this interesting chromophore.[1−3] One group of complexes that has received much attention in recent years is the class of complexes that contain polyazine bridging ligands.[3−15] The presence of these bridging ligands allows for the incorporation of multiple metal centers into one molecule allowing for the construction of complex supramolecular species. One of the most highly studied bidentate bridging ligands is dpp (2,3-bis(2-pyridyl)pyrazine).[4−9,10a−d,11,12,14,15] Interest in this ligand arises from its ability to form stable polymetallic complexes

[†] Current address: National Institute of Materials and Chemical Research, 1-1 Higashi, Tsukuba, Ibaraki 305, Japan.

[‡] E-mail: kbrewer@chemserver.chem.vt.edu.

[⊗] Abstract published in *Advance ACS Abstracts,* June 1, 1997.

(1) Juris, A.; Balzani, V.; Barigelletti, F.; Campagna, S.; Belser, P.; von Zelewsky, A. *Coord. Chem. Rev.* **1988**, *84*, 85.

(2) Kalyanasundaram, K. *Coord. Chem. Rev.* **1982**, *46*, 159.

(3) (a) Meyer, T. J. *Pure Appl. Chem.* **1986**, *58*, 1576. (b) Durham, B.; Caspar, J. V.; Nagle, J. K.; Meyer, T. J. *J. Am. Chem. Soc.* **1982**, *104*, 4803. (c) Strouse, G. F.; Schoonover, J. R.; Duesing, R.; Boyde, S.; Jones, W. E.; Meyer, T. J. *Inorg. Chem.* **1995**, *34*, 473. (d) Anderson, P. A.; Strouse, G. F.; Treadway, J. A.; Keene, F. R.; Meyer, T. J. *Inorg. Chem.* **1994**, *33*, 3863.

(4) For a recent review, see: Balzani, V.; Juris, A.; Venturi, M.; Campagna, S.; Serroni, S. *Chem. Rev.* **1996**, *96*, 759.

(5) (a) Denti, G.; Campagna, S.; Serroni, S.; Ciano, M.; Balzani, V. *J. Am. Chem. Soc.* **1992**, *114*, 2944. (b) Campagna, S.; Denti, G.; Serroni, S.; Ciano, M.; Balzani, V. *Inorg. Chem.* **1991**, *30*, 3728.

(6) (a) Campagna, S.; Denti, G.; Sabatino, L.; Serroni, S.; Ciano, M.; Balzani, V. *Gazz. Chim. Ital.* **1989,** *119*, 415. (b) Juris, A.; Balzani, V.; Campagna, S.; Denti, G.; Serroni, S.; Frei, G.; Gudel, H. U. *Inorg. Chem.* **1994,** *33*, 1491. (c) Denti, G.; Campagna, S.; Sabatino, L.; Ciano, M.; Balzani, V. *Inorg. Chem.* **1990**, *29*, 4750. (d) Campagna, S.; Denti, G.; Serroni, S.; Juris, A.; Venturi, M.; Ricevuto, V.; Balzani, V. *Chem. Eur. J.* **1995**, *1*, 211. (e) Juris, A.; Venturi, M.; Pontoni, L.; Resino, I.; Balzani, V.; Serroni, S.; Campagna, S.; Denti, G. *Can J. Chem.* **1995**, *73*, 1875.

(7) Serroni, S.; Denti, G. *Inorg. Chem.* **1992**, *31*, 4251.

(8) (a) Balzani, V.; Moggi, L. *Coord. Chem. Rev.* **1990**, *97*, 313. (b) Balzani, V. *J. Photochem. Photobiol.* **1990**, *51*, 55. (c) Balzani, V.; Moggi, L.; Scandola, F. In *Supramolecular Photochemistry*; Balzani, V., Ed.; NATO ASI Series 214; Reidel: Dordrecht, The Netherlands, 1987; p 1. (d) Balzani, V.; Credi, A.; Scandola, F. In *Transition Metals in Supramolecular Chemistry;* Fabbrizzi, L., Poggi, A., Eds.; Kluwer Academic Publishers: Dordrecht, The Netherlands, 1994; p 1.

(9) Serroni, S.; Campagna, S.; Denti, G.; Keyes, T. E.; Vos, J. G. *Inorg. Chem.* **1996,** *35*, 4513.

(10) (a) Bridgewater, J. S.; Vogler, L. M.; Molnar, S. M.; Brewer, K. J. *Inorg. Chim. Acta* **1993**, *208*, 179. (b) Richter, M. M.; Brewer, K. J. *Inorg. Chem.* **1993**, *22*, 2827. (c) Richter, M. M.; Brewer, K. J. *Inorg. Chem.* **1993**, *22*, 5762. (d) Molnar, S. M.; Jensen, G. E.; Vogler, L. M.; Jones, S. W.; Laverman, L.; Bridgewater, J. S.; Richter, M. M.; Brewer, K. J. *J. Photochem. Photobiol. A: Chem.* **1994**, *80*, 315. (e) Molnar, S. M.; Nallas, G. N.; Bridgewater, J. S.; Brewer, K. J. *J. Am. Chem. Soc.* **1994**, *116*, 5206. (f) Milkevitch, M.; Brauns, E.; Brewer, K. J. *Inorg. Chem.* **1996**, *35*, 1737. (g) Vogler, L. M.; Brewer, K. J. *Inorg. Chem.* **1996**, *35*, 818. (f) Nallas, G. N.; Jones, S. W.; Brewer, K. J. *Inorg. Chem.* **1996**, *35*, 6974.

(11) (a) Brewer, K. J.; Murphy, W. R.; Spurlin, S. R.; Petersen, J. D. *Inorg. Chem.* **1986**, *25*, 882. (b) Petersen, J. D. In *Supramolecular Photochemistry*; Balzani, V., Ed.; NATO ASI Series 214; Reidel: Dordrecht, *The Netherlands*, 1987; p 135. (c) Ruminski, R. R.; Petersen, J. D. *Inorg. Chem.* **1982**, *21*, 3706. (d) Ruminski, R. R.; Petersen, J. D. *Inorg. Chim. Acta* **1985**, *97*, 129. (e) MacQueen, D. B.; Petersen, J. D. *Inorg. Chem.* **1990**, *29*, 2313. (f) Cooper, J. B.; MacQueen, D. B.; Petersen, J. D.; Wertz, D. W. *Inorg. Chem.* **1990**, *29*, 3701.

(12) (a) Fuchs, Y.; Lofters, S.; Dieter, T.; Shi, W.; Morgan, S.; Strekas, T. C.; Gafney, H. D.; Baker, A. D. *J. Am. Chem. Soc.* **1987**, *109*, 2691. (b) Braunstein, C. H.; Baker, A. D.; Strekas, T. C.; Gafney, H. D. *Inorg. Chem.* **1984**, *23*, 857.

(13) (a) Rillema, D. P.; Taghdiri, G. D.; Jones, D. S.; Keller, C. D.; Worl, L. A.; Meyer, T. J.; Levy, H. A. *Inorg. Chem.* **1987**, *26*, 578. (b) Sahai, R.; Morgan, L.; Rillema, D. P. *Inorg. Chem.* **1988**, *27*, 3495. (c) Rillema, D. P.; Callahan, R. W.; Mack, K. B. *Inorg. Chem.* **1982**, *21*, 2589.

(14) Kalyanasundaram, K.; Gratzel, M.; Nazeeruddin, Md. K. *J. Phys. Chem.* **1992**, *96*, 5865.

(15) Berger, R. M. *Inorg. Chem.* **1990**, *29*, 1920.

S0020-1669(96)01302-X CCC: $14.00

which typically display observable emissions at room temperature. In an elegant manuscript in 1987, Balzani et al. proposed a vast array of molecular devices with widely varied functions that might be constructed from these and related chromophores.[8c] Recent interest in polymetallic complexes arises from the ability to couple different types of metal complexes with varied chemical properties that can lead to the construction of supramolecular species.[4−10] Use of the dpp bridging ligand alone has drawbacks in the preparation of molecular devices which function as charge separation or electron collection devices. The dpp ligand can sometimes display a lack of stability in its reduced form, particularly in mixed-metal systems.[10a−c,11f,15] In addition, using the same bridging ligand throughout a device does not allow for the varied orbital energies often desired in many types of devices.[4,8,10]

A wide variety of polymetallic complexes incorporating the polyazine bridging ligand dpp have been reported.[4−9,10a−d,11,12,14,15] Balzani et al. have utilized the "complexes-as-ligands" and "complexes-as-metals" synthetic strategies to prepare many interesting large supramolecular complexes.[4−9] Recently, a paper appeared that described a unique tetranuclear ruthenium complex that contained both the dpp and bpt bridging ligands (Hbpt = 3,5-bis(pyridyn-2-yl)-1,2,4-triazole).[9] Our group has studied a series of trimetallic complexes using the bidentate bridging ligands dpp, dpq, and dpb (dpq = 2,3-bis(2-pyridyl)-quinoxaline and dpb = 2,3-bis(2-pyridyl)benzoquinoxaline).[10a−e] The dpq and dpb systems tend to be quite stable in their reduced forms, and the $[\{(bpy)_2Ru(dpb)\}_2IrCl_2]^{5+}$ complex has been shown to be the first functioning molecular device for photoinitiated electron collection.[10a,d,e] One drawback of the dpq and dpb ligands is the lower energy MLCT states relative to the analogous dpp-bridged systems.[4,10,12,13] This gives rise to polymetallic complexes with very short MLCT excited state lifetimes.

One set of the synthons often utilized in the preparation of supramolecular complexes using the dpp bridging ligand are $[\{(bpy)_2M(dpp)\}_2RuCl_2]^{4+}$ (M = Ru^{II} or Os^{II}).[5] The preparation of these very useful synthons appears in the literature, and preliminary spectroscopic and electrochemical data is given.[5] For M = Ru the complex has a lowest lying absorption at 618 nm, and this transition occurs at 600 nm for M = Os. Both systems display a central Ru that oxidizes first at 0.72 and 0.75 V vs SCE (saturated calomel electrode) for the Ru and Os system, respectively. The terminal metals display an overlapping oxidation at 1.45 and 1.15 V for the Ru- and Os-based systems, respectively. Herein, these trimetallic species will serve as useful building blocks for the construction of a new class of synthetically useful supramolecular light absorbers by the coupling of a dpq ligand to produce $[\{(bpy)_2M(dpp)\}_2Ru(dpq)]^{6+}$. This will give rise to chromophores which can later be incorporated into a wide array of supramolecular systems. These new supramolecular systems will have two $(bpy)_2M^{II}(dpp)$ chromophores but also possess a terminal dpq ligand. Once the dpq forms a bridge, upon incorporation into larger supramolecular species, the LUMO (lowest unoccupied molecular orbital) will reside on the π^* orbital of the bridging dpq ligand.[10,12,13] The details of the preparation of these complexes, as well as the spectroscopic, electrochemical, and spectroelectrochemical analysis of these new light absorbers and the dichloro synthons, is reported herein.

Experimental Section

$[\{(bpy)_2Ru(dpp)\}_2RuCl_2](PF_6)_4$ was synthesized by a modification of a previously published preparation.[5] $RuCl_3 \cdot 3H_2O$ (0.014 g, 0.053 mmol), $[Ru(bpy)_2(dpp)](PF_6)_2$ (0.079 g, 0.084 mmol), and LiCl (0.018 g, 0.43 mmol) were heated at reflux in 15 mL of 95% EtOH under argon for 7.5 h. The reaction mixture was cooled to room temperature, and 50 mL of saturated aqueous KPF_6 was added to induce precipitation. The crude product was filtered, dissolved in minimal acetonitrile, added to ethanol, and cooled overnight at 15 °C. The precipitate was filtered and washed with ethanol and diethyl ether. The desired dichloro species can be purified by column chromatography using adsorption alumina and a 1:1 toluene:acetonitrile solvent mixture. Yield: 66%. FAB-MS *m/z* (relative abundance, ion): 1902 (50, $[\{(bpy)_2Ru(dpp)\}_2RuCl_2](PF_6)_3^+$), 1757 (100, $[\{(bpy)_2Ru(dpp)\}_2RuCl_2](PF_6)_2^+$), 1612 (45, $[\{(bpy)_2Ru(dpp)\}_2RuCl_2](PF_6)^+$).

$[\{(bpy)_2Ru(dpp)\}_2Ru(dpq)](PF_6)_6$ was prepared by the reaction of the chloro complex $[\{(bpy)_2Ru(dpp)\}_2RuCl_2](PF_6)_4$ (0.30 g, 0.15 mmol) and dpq (0.23 g, 0.81 mmol) at reflux under nitrogen in 15 mL of 2:1 ethanol:water for 36 h. The reaction mixture was cooled to room temperature, and the crude product was precipitated as the PF_6^- salt by addition to 100 mL of saturated aqueous KPF_6. The precipitate was collected by vacuum filtration. Purification was achieved on a LH20 size exclusion column using 2:1 ethanol:acetonitrile as the mobile phase. The major (red) band was collected, and the solvent was removed by rotary evaporation. The product was dissolved in minimal acetonitrile, flash precipitated in 100 mL of diethyl ether, and collected by vacuum filtration. Yield: 55%. FAB-MS: *m/z* (relative abundance, ion): 2406 (50, $[\{(bpy)_2Ru(dpp)\}_2Ru(dpq)](PF_6)_5^+$), 2261 (100, $[\{(bpy)_2Ru(dpp)\}_2Ru(dpq)](PF_6)_4^+$), 2116 (70, $[\{(bpy)_2Ru(dpp)\}_2Ru(dpq)](PF_6)_3^+$).

$[\{(bpy)_2Os(dpp)\}_2RuCl_2](PF_6)_4$ was prepared by a modification of the literature preparation.[5] $RuCl_3 \cdot 3H_2O$ (0.026 g, 0.10 mmol), $[Os(bpy)_2(dpp)](PF_6)_2$ (0.21 g, 0.20 mmol), and LiCl (0.025 g, 0.61 mmol) were heated at reflux in 30 mL of EtOH under argon for 8.5 h. The reaction mixture was cooled to room temperature, and saturated aqueous KPF_6 (60 mL) was added to induce precipitation. The crude product was filtered, dissolved in minimal acetonitrile, and precipitated in diethyl ether. Purification was achieved by LH20 size exclusion column chromatography with 2:1 ethanol:acetonitrile as the mobile phase. Yield: 67%. FAB-MS: *m/z* (relative abundance, ion): 2080 (50, $[\{(bpy)_2Os(dpp)\}_2RuCl_2](PF_6)_3^+$), 1935 (100, $[\{(bpy)_2Os(dpp)\}_2RuCl_2](PF_6)_2^+$), 1790 (57, $[\{(bpy)_2Os(dpp)\}_2RuCl_2](PF_6)^+$).

$[\{(bpy)_2Os(dpp)\}_2Ru(dpq)](PF_6)_6$ was prepared by the reaction of the dichloro precursor $[\{(bpy)_2Os(dpp)\}_2RuCl_2](PF_6)_4$ (0.15 g, 0.062 mmol) with $AgCF_3SO_3$ (0.039 g, 0.15 mmol) in 8 mL of 95% ethanol at reflux in the dark for 3 h to produce the solvato complex and a AgCl precipitate that was removed by gravity filtration. Ethylene glycol (8 mL) and dpq (0.18 g, 0.62 mmol) were added, and the reaction mixture was heated for an additional 22 h. The reaction mixture was cooled to room temperature and added to 50 mL of saturated aqueous KPF_6 to induce precipitation. The crude product was collected by vacuum filtration, dissolved in minimal acetonitrile, precipitated by addition to diethyl ether, and collected by vacuum filtration. Purification was achieved on an LH20 size exclusion column using 2:1 ethanol: acetonitrile as the mobile phase. The major (red) band was collected, and the solvent was removed by rotary evaporation. The product was dissolved in minimal acetonitrile, flash precipitated in 100 mL of diethyl ether, and collected by vacuum filtration. Yield: 56%. FAB-MS: *m/z* (relative abundance, ion): 2439 (75, $[\{(bpy)_2Os(dpp)\}_2Ru(dpq)](PF_6)_4^+$), 2294 (100, $[\{(bpy)_2Os(dpp)\}_2Ru(dpq)](PF_6)_3^+$), 2149 (50, $[\{(bpy)_2Os(dpp)\}_2Ru(dpq)](PF_6)_2^+$).

Fast Atom Bombardment (FAB) Mass Spectral Analysis. FAB mass spectral analysis was conducted on these trimetallic complexes using *m*-nitrobenzyl alcohol as the matrix, with a small amount of acetonitrile added to facilitate analyte dissolution. The analysis was conducted on a Fisons VG Quattro triple-stage quadrupole mass spectrophotometer. The trimetallic complexes give very nice fragmentation patterns, with a series of ions with the trimetallic core intact and varied numbers of PF_6^- counterions being observed.

Electronic Absorption Spectroscopy. The electronic absorption spectroscopy of these complexes was collected at room temperature on acetonitrile solutions that were prepared gravimetrically. Spectra were recorded using a HP 8452A diode array spectrophotometer with 2 nm resolution.

Emission Spectroscopy and Excited State Lifetime Measurements. Emission spectra were recorded at room temperature in deoxygenated CH_3CN using a PTI Alphascan fluorometer modified to

detect red-shifted emissions with a thermoelectrically cooled Hamamatsu R666S photomultiplier tube (PMT). Emission spectra were not corrected for PMT response. Emission lifetimes were determined using a PTI PL 2300 nitrogen laser with a tunable dye head as the pulsed excitation source. The time profile of the emission was collected at right angles to the excitation using a Hamamatsu R928 PMT and a LeCroy 6880B digital oscilloscope. The data were fit to a single-exponential function after discarding the initial points that contain the laser pulse, $Y = A + B(\exp(-X/c))$ where $c = \tau$ in s.

Electrochemistry. Cyclic voltammetric measurements were carried out on millimolar solutions of the analyte in Burdick and Jackson UV grade acetonitrile that contained 0.1 M Bu_4NPF_6 as the supporting electrolyte. Our electrochemical system consisted of a BAS 100W electrochemical analyzer that utilized a Pt disk working (2.0 mm^2), Pt wire auxiliary, and Ag/AgCl reference electrode (0.29 V vs NHE (normal hydrogen electrode) calibrated vs Fc/Fc^+ ($E_{1/2}$ = 0.665 V vs NHE[16])). Measurements were made at a scan rate of 200 mV/s, and the working electrode was manually cleaned prior to each analysis.

Spectroelectrochemistry. Spectroelectrochemistry was conducted on acetonitrile solutions that were ca. 5×10^{-6} M in analyte and contained 0.1 M Bu_4NPF_6 as the supporting electrolyte, using a previously described spectroelectrochemical cell of local design and construction.[17,18] The modified H-cell uses a 1-cm quartz cuvette as the working compartment, a Pt mesh as the working electrode, and a Pt mesh auxiliary electrode. The reference electrode is housed in a separate compartment connected to the working compartment by a fine porosity glass frit. All electrolyses were continued until no further change in the electronic absorption spectroscopy was observed (±2%). The reversibility of the electrochemical transformation was ascertained by a subsequent electrolyses to the original oxidation state and analysis of the electronic absorption spectrum. The region of the spectrum exhibiting the lowest return is used to report the percentage reversibility of the redox process under these conditions.

Results and Discussion

Synthesis. The preparation of the dichloro complexes, $[\{(bpy)_2M(dpp)\}_2RuCl_2]^{4+}$ (M = Os^{II} or Ru^{II}), was adapted from the literature.[5] Our synthetic method for the preparation of the new terminal dpq complexes, $[\{(bpy)_2M(dpp)\}_2Ru(dpq)]^{6+}$ (M = Os^{II} or Ru^{II}), is shown in Scheme 1. These complexes are prepared by direct reaction of the dpq ligand with the appropriate dichloro starting material. This is in contrast to the elegant protection−deprotection synthetic scheme developed for the preparation of the analogous terminal dpp systems $[\{(bpy)_2Ru(dpp)\}_2Ru(dpp)]^{6+}$.[7] FAB-MS analyses were utilized in characterizing these complexes. These trimetallic species gave nice FAB-MS data, with ions appearing associated with the trimetallic core intact and varying numbers of PF_6^- counterions.

Electrochemistry. The electrochemistry of these four trimetallic complexes is summarized in Table 1. Complexes of this type typically possess metal-based oxidations and ligand-localized reductions for each polyazine ligand.[4−15] In addition, bridging dpp ligands have been shown to undergo two sequential one-electron reductions prior to the reduction of the terminal bpy ligands in polymetallic complexes of ruthenium and osmium.[4,10,11f,15]

The cyclic voltammetry of the $[\{(bpy)_2M(dpp)\}_2RuCl_2]^{4+}$ species shows the two previously reported oxidations[5] and four reductions. Passing through the fourth reduction leads to adsorption of the electrogenerated neutral complex onto the electrode surface and makes further electrochemical analysis difficult. Oxidatively, each $[\{(bpy)_2M(dpp)\}_2RuCl_2]^{4+}$ species displays two reversible waves, with the first couple displaying half the peak current of the second couple.[5] The first oxidation, representing the oxidation of one metal center, occurs at 0.83 V for $[\{(bpy)_2Ru(dpp)\}_2RuCl_2]^{4+}$ and 0.78 V for $[\{(bpy)_2Os(dpp)\}_2RuCl_2]^{4+}$, confirming its assignment as being due to the $(\mu\text{-dpp})_2Ru^{II}Cl_2$ moiety. The second oxidation at 1.60 and 1.21

Scheme 1

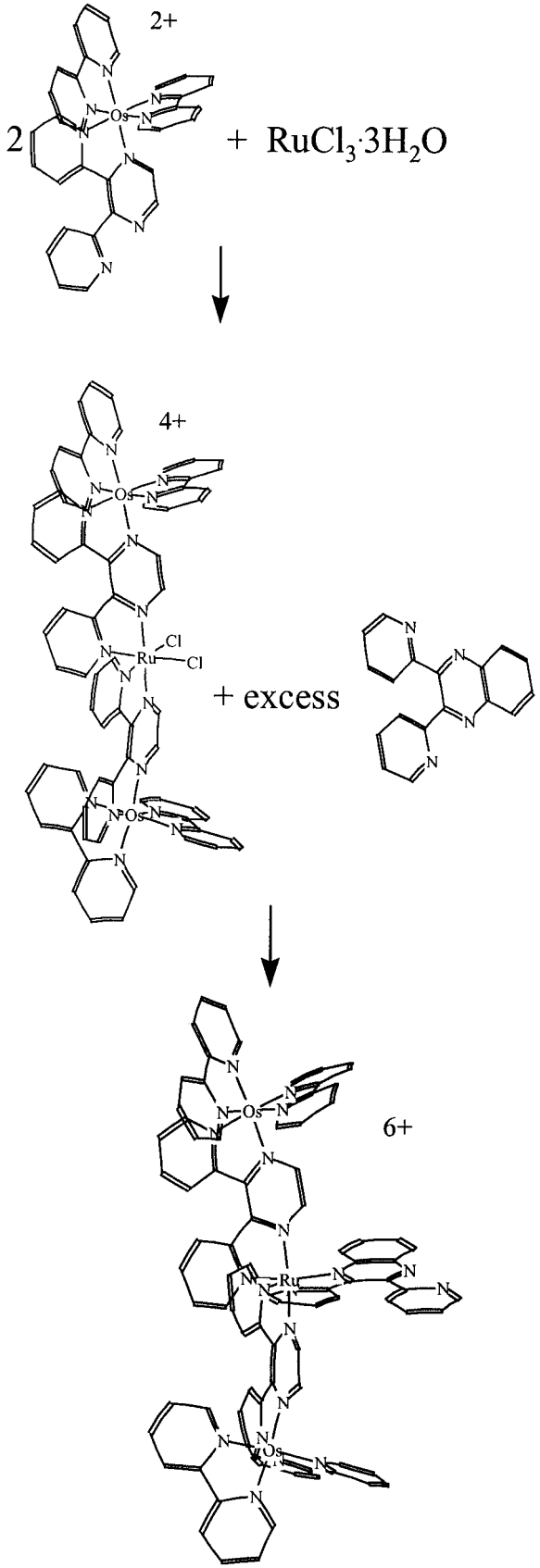

(16) Gennett, G. A.; Yellowless, L. J.; Braterman, P. S. *J. Chem. Soc., Chem. Commun.* **1981**, 287.
(17) Jones, S. W.; Vrana, L. M.; Brewer, K. J. *J. Organomet. Chem.* **1997**, in press.
(18) Brewer, K. J.; Calvin, M.; Lumpkin, R. S.; Otvos, J. W.; Spreer, L. O. *Inorg. Chem.* **1989**, *28*, 4446.

Table 1. Electrochemical Data for a Series of Polyazine-Bridged Trimetallic Complexes of the Form $[\{(bpy)_2M(dpp)\}_2RuCl_2]^{4+}$ and $[\{(bpy)_2M(dpp)\}_2Ru(dpq)]^{6+}$ (M = Ru^{II} or Os^{II})[a]

	$E_{1/2}$ (V vs Ag/AgCl)[b]	
complex	oxidations (assignment)	reductions (assignment)
$[\{(bpy)_2\mathbf{Ru}(dpp)\}_2RuCl_2]^{4+}$ [d]	0.83 (Ru^{II}/Ru^{III}) 1.60 ($2\mathbf{Ru}^{II}/2\mathbf{Ru}^{III}$)	−0.71 (dpp,dpp/dpp^-,dpp) −0.88 (dpp^-,dpp/dpp^-,dpp^-) −1.43[c] (dpp^-,dpp^-/dpp^{2-},dpp^-) −1.52[c] (dpp^{2-},dpp^-/dpp^{2-},dpp^{2-})
$[\{(bpy)_2Os(dpp)\}_2RuCl_2]^{4+}$ [d]	0.78 (Ru^{II}/Ru^{III}) 1.21 ($2Os^{II}/2Os^{III}$)	−0.70 (dpp,dpp/dpp^-,dpp) −0.84 (dpp^-,dpp/dpp^-,dpp^-) −1.30[c] (dpp^-,dpp^-/dpp^{2-},dpp^-) −1.40[c] (dpp^{2-},dpp^-/dpp^{2-},dpp^{2-})
$[\{(bpy)_2\mathbf{Ru}(dpp)\}_2Ru(dpq)]^{6+}$	1.66 ($2\mathbf{Ru}^{II}/2\mathbf{Ru}^{III}$)	−0.36 (dpp,dpp/dpp^-,dpp) −0.52 (dpp^-,dpp/dpp^-,dpp^-) −0.76 (dpq/dpq^-) −1.13 (dpp^-,dpp^-/dpp^{2-},dpp^-) −1.28 (dpp^{2-},dpp^-/dpp^{2-},dpp^{2-}) −1.41[c] (dpq^-/dpq^{2-})
$[\{(bpy)_2Os(dpp)\}_2Ru(dpq)]^{6+}$	1.18 ($2Os^{II}/2Os^{III}$)	−0.47 (dpp,dpp/dpp^-,dpp) −0.59 (dpp^-,dpp/dpp^-,dpp^-) −0.80 (dpq/dpq^-) −1.18 (dpp^-,dpp^-/dpp^{2-},dpp^-) −1.28 (dpp^{2-},dpp^-/dpp^{2-},dpp^{2-}) −1.45[c] (dpq^-/dpq^{2-})

[a] Where bpy = 2,2′-bipyridine, dpp = 2,3-bis(2-pyridyl)pyrazine, and dpq = 2,3-bis(2-pyridyl)quinoxaline. [b] Measured in CH_3CN with 0.1 M Bu_4NPF_6 as the supporting electrolyte at 200 mV/s using a Ag/AgCl reference electrode (0.29 V vs NHE calibrated vs Fc/Fc^+ [16]). [c] E_p^c reported due to poor resolution from adsorption onto the electrode surface. [d] The oxidative electrochemistry has been previously reported (ref 5), but the numbers given are measured under our conditions to make comparisons more valid.

V for $[\{(bpy)_2Ru(dpp)\}_2RuCl_2]^{4+}$, and $[\{(bpy)_2Os(dpp)\}_2RuCl_2]^{4+}$, respectively, represents two overlapping one-electron oxidations of the terminal $(bpy)_2M^{II}(\mu\text{-dpp})$ (M = Ru or Os) centers, consistent with the previously reported oxidative electrochemistry.[5] The terminal metals in the osmium-based complex are 390 mV easier to oxidize than the terminal metals in the ruthenium-based system, consistent with the higher energy dπ orbitals on osmium and the M^{II}/M^{III} assignment. The reductive processes for $[\{(bpy)_2M(dpp)\}_2RuCl_2]^{4+}$ appear as two sets of two closely spaced waves that occur at a similar potential for the Os- and Ru-based trimetallic systems. These represent the reduction of the bridging dpp ligands by one and then two electrons. These equivalent dpp ligands reduce at slightly different potentials since they are influenced by each other. Each dpp ligand is reduced by two electrons prior to the reduction of the terminal bpy ligands, consistent with the polymetallic formulation of these complexes.[4,10,11f,15] It is not possible to resolve the bpy reductions due to the absorption of the four-electron reduction product on the electrode surface.

These $[\{(bpy)_2M(dpp)\}_2RuCl_2]^{4+}$ complexes have Ru(dπ)-based HOMOs (highest occupied molecular orbitals) and dpp-based LUMOs. This is expected to lead to lowest lying excited states that are Ru(dπ) → dpp(π^*) charge transfer (CT) in nature. These excited states should be at relatively similar energy for the two systems, M = Ru or Os, consistent with the previously reported spectroscopy.[5]

The cyclic voltammetry of the $[\{(bpy)_2M(dpp)\}_2Ru(dpq)]^{6+}$ species shows one oxidation and five well-behaved reductions. Scanning negative of the fifth reduction leads to adsorption of the neutral complex onto the electrode surface and adsorption and desorption spikes in the cyclic voltammogram. In both complexes, the oxidative wave represents two closely spaced and overlapping one-electron processes. This couple shifts from 1.66 V in $[\{(bpy)_2Ru(dpp)\}_2Ru(dpq)]^{6+}$ to 1.18 V in $[\{(bpy)_2Os(dpp)\}_2Ru(dpq)]^{6+}$, indicative of its M^{II}/M^{III}-based nature for the $(bpy)_2M(\mu\text{-dpp})$ metal center. The oxidation of the $(\mu\text{-dpp})_2Ru^{II}(dpq)$ metal center is not observed within our solvent window. This metal, which is bound to three polyazine bridging ligands, two acting in a bridging capacity, should be relatively electron deficient compared to the $(bpy)_2M^{II}(\mu\text{-dpp})$ metal centers in these complexes and, thus, is expected to be difficult to oxidize.[4,10,12,13] The $[\{(bpy)_2Ru(dpp)\}_2Ru(dpq)]^{6+}$ and $[\{(bpy)_2Os(dpp)\}_2Ru(dpq)]^{6+}$ complexes possess two closely spaced reductive couples at −0.36 and −0.52 V and −0.47 and −0.59 V, respectively. These couples represent the one-electron reduction of each bridging dpp ligand. These equivalent dpp ligands reduce at slightly different potentials since they are influenced by each other. The potential of these reductions does not vary significantly as the terminal metal is varied from Ru to Os. This is consistent with the ligand-based nature of these processes. Closely following these dpp couples is a single wave that represents the reduction of the terminal dpq ligand, dpq/dpq^-. This wave occurs at −0.76 and −0.80 V, respectively, for $[\{(bpy)_2Ru(dpp)\}_2Ru(dpq)]^{6+}$ and $[\{(bpy)_2Os(dpp)\}_2Ru(dpq)]^{6+}$. Typically, bridging dpp ligands exhibit two reductions prior to the reduction of terminal ligands within a polymetallic framework.[4,11f,15] This is true for systems possessing terminal bpy ligands like the well-studied $[(bpy)_2Ru(dpp)Ru(bpy)_2]^{4+}$ [11f,15] and the above-discussed $[\{(bpy)_2Ru(dpp)\}_2RuCl_2]^{4+}$.[5] In the case of these dpq systems, $[\{(bpy)_2Ru(dpp)\}_2Ru(dpq)]^{6+}$ and $[\{(bpy)_2Os(dpp)\}_2Ru(dpq)]^{6+}$, the terminal ligand is dpq, which is significantly easier to reduce than bpy.[4,10,12] This gives rise to a positive shift in the reduction potential for this ligand, placing the dpq/dpq^- couple at a potential positive of the $\mu\text{-dpp}^-/\mu\text{-dpp}^{2-}$ couples. This type of behavior is reported in the literature for $[(biq)_2Ru(dpp)Ru(biq)_2]^{4+}$, in which the biq/$biq^-$ wave appears prior to the $\mu\text{-dpp}^-/\mu\text{-dpp}^{2-}$ couple.[6c] Both $[\{(bpy)_2Ru(dpp)\}_2Ru(dpq)]^{6+}$ and $[\{(bpy)_2Os(dpp)\}_2Ru(dpq)]^{6+}$ display a second set of dpp reductions, i.e., dpp^-/dpp^{2-} at −1.13 and −1.28 V and −1.18 and −1.28 V, respectively. These dpp^-/dpp^{2-} couples appear as sets of two closely spaced waves. Further reduction of the terminal dpq ligand and reduction of the bpy ligands follows but is obscured by adsorption of the complex onto the electrode surface. A similar complex with a terminal bpy ligand, $[\{(bpy)_2Ru(dpp)\}_2Ru(bpy)]^{6+}$, has been reported by Balzani, Denti, Campagna et al. and its electrochemical properties given.[6c] This complex shows one oxidation at 1.48 V corresponding to the two $(bpy)_2Ru^{II}(\mu\text{−dpp})$ moieties

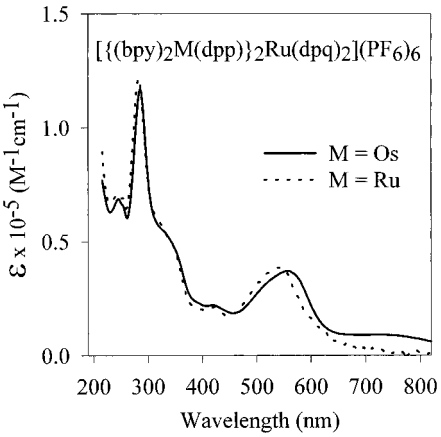

Figure 1. Electronic absorption spectroscopy of a series of trimetallic complexes of the form $[\{(bpy)_2M(dpp)\}_2Ru(dpq)]^{6+}$ measured in CH_3CN at room temperature (M = Ru^{II} or Os^{II}, bpy = 2,2′-bipyridine, dpp = 2,3-bis(2-pyridyl)pyrazine, and dpq = 2,3-bis(2-pyridyl)-quinoxaline).

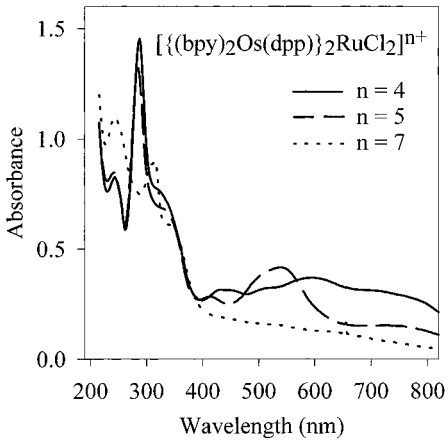

Figure 2. Spectroelectrochemistry of $[\{(bpy)_2Os(dpp)\}_2RuCl_2]^{4+}$ measured in a 0.1 M Bu_4NPF_6 CH_3CN solution at room temperature (bpy = 2,2′-bipyridine, and dpp = 2,3-bis(2-pyridyl)pyrazine).

and a series of reductions at −0.55, −0.75, −1.17, and −1.47 V vs SCE. This electrochemistry is quite similar to the Ru- and dpp-based waves for our $[\{(bpy)_2Ru(dpp)\}_2Ru(dpq)]^{6+}$ complex.

Our $[\{(bpy)_2M(dpp)\}_2Ru(dpq)]^{6+}$ complexes have M(dπ)-based HOMOs and dpp-based LUMOs. This is expected to lead to lowest lying excited states that are M(dπ) → dpp(π*) CT in nature. This excited state should vary in energy as a function of the nature of the terminal metal, Os or Ru, with the Os-based system displaying the lowest lying MLCT state.

Spectroscopy. The electronic absorption spectroscopy for the $[\{(bpy)_2M(dpp)\}_2Ru(dpq)]^{6+}$ (M = Ru^{II} or Os^{II}) complexes are illustrated in Figure 1. The spectroscopy of polyazine-bridged complexes is dominated by MLCT transitions in the visible and ligand-based $\pi \rightarrow \pi^*$ and n → π^* transitions in the UV.[4−15] MLCT transitions are typically observed for each chromophoric metal center and each coordinated polyazine acceptor ligand. In complexes with bridging dpp and terminal bpy ligands, the MLCT transitions that involve the bridging dpp ligand occur at lower energy than the analogous transitions for the bpy acceptor ligands due to the lower energy π^* orbitals on dpp.[4,12] Ligand-based $\pi \rightarrow \pi^*$ transitions can typically be observed for each polyazine ligand.

The spectroscopy of the terminal chloride complexes, $[\{(bpy)_2M(dpp)\}_2RuCl_2]^{4+}$, contains many similar bands for the osmium- and ruthenium-based complexes with an increase in absorbance in the low-energy tail (650−800 nm) for the osmium analog. Both of these complexes are expected to possess a lowest energy ^{1}MLCT that is Ru(dπ) → dpp(π^*) CT in nature for the central Ru bound to the two dpp and two chloride ligands that occurs at 600 and 620 nm for the Os- and Ru-based systems, respectively, consistent with the literature values.[5] A higher energy band appears at 512 and 496 nm in the Os- and Ru-based systems, respectively, and represents the M(dπ) → dpp(π^*) CT band for the terminal M units. The 430 nm region of the spectrum of both complexes exhibits another transition that is assigned as a M(dπ) → bpy(π^*) CT band based on the spectroscopy of other dpp-bridged species with terminal bpy ligands.[4,12] The UV region contains an intense band at 292 nm for both complexes that represents a bpy-based $\pi \rightarrow \pi^*$ transition.[4,10,12] A lower energy shoulder appears at ca. 330 nm for both complexes and represents the dpp-based $\pi \rightarrow \pi^*$ transition. The 650−800 nm region of the spectrum for the osmium complex exhibits increased absorbance relative to the ruthenium analog. This likely results from the expected ^{3}MLCT transitions that will occur in this region, having increased intensity in the osmium analogs due to the higher degree of spin−orbit coupling.

The spectroscopy of the terminal dpq complexes, $[\{(bpy)_2M(dpp)\}_2Ru(dpq)]^{6+}$, contains many similar bands for the osmium- and ruthenium-based complexes, with minor increases in absorbance for the osmium-based system in the 650−800 nm region. The UV region is quite similar to the terminal chloride systems described above, with bpy- and dpp-based $\pi \rightarrow \pi^*$ transitions occurring at 292 and 330 nm, respectively. The M(dπ) → bpy(π^*) CT transition appears at 420 nm for both complexes. The lowest energy transition is now expected to be the M(dπ) → dpp(π^*) CT band, which is centered at 560 and 540 nm for the osmium- and ruthenium-based systems, respectively. This peak occurs at a very similar energy to that reported by Balzani et al. for the terminal bpy complex, $[\{(bpy)_2Ru(dpp)\}_2Ru(bpy)]^{6+}$.[6c] The low energy tail at 650−800 nm in $[\{(bpy)_2Os(dpp)\}_2Ru(dpq)]^{6+}$ represents the ^{3}MLCT bands expected to occur in this region and give rise to an increase in absorbance for the osmium complex relative to its ruthenium analog. Our $[\{(bpy)_2M(dpp)\}_2Ru(dpq)]^{6+}$ complexes should also display a Ru(dπ) → dpq(π^*) CT band in the 500−520 nm region, which appears as a higher energy shoulder on the more intense M(dπ) → dpp(π^*) CT band.[4,13]

The $[\{(bpy)_2Ru(dpp)\}_2Ru(dpq)](PF_6)_6$ system displays an observable emission at room temperature in CH_3CN solution. The osmium analog and the dichloro species do not display an emission that is observable on our fluorometer. Those trimetallics would be expected to have a lower energy emission than $[\{(bpy)_2Ru(dpp)\}_2Ru(dpq)]^{6+}$, which is near the low-energy detection limit for our system. The $[\{(bpy)_2Ru(dpp)\}_2Ru(dpq)](PF_6)_6$ system displays an emission with a maximum at 775 nm and a lifetime of 65 ns at room temperature in deoxygenated CH_3CN solution. This is quite similar to the 804 nm emission and 80 ns lifetime of the terminal bpy complex, $[\{(bpy)_2Ru(dpp)\}_2Ru(bpy)]^{6+}$, previously reported in the literature.[6c] This emission from our $[\{(bpy)_2Ru(dpp)\}_2Ru(dpq)](PF_6)_6$ species is consistent with the Ru(dπ) → dpp(π^*) CT nature of the lowest lying excited state. This is predicted by the electrochemistry, which shows the expected lower energy π^* orbital for the bridging dpp versus the terminal dpq ligand.[4,6,12,13]

Spectroelectrochemistry. The oxidative spectroelectrochemistry data for the $[\{(bpy)_2M(dpp)\}_2RuCl_2]^{4+}$ and $[\{(bpy)_2M(dpp)\}_2Ru(dpq)]^{6+}$ complexes are illustrated in Figures 2−5. It was not possible to reversibly reduce these complexes. This is consistent with the dpp-based nature of the LUMO of these species.[10a−c,11f,15] It was possible to generate the oxidized forms

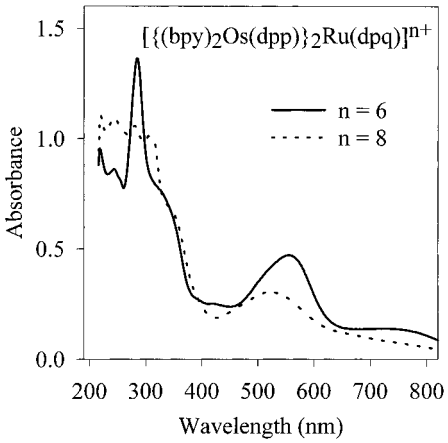

Figure 3. Spectroelectrochemistry of $[\{(bpy)_2Os(dpp)\}_2Ru(dpq)]^{6+}$ measured in a 0.1 M Bu_4NPF_6 CH_3CN solution at room temperature (bpy = 2,2′-bipyridine, dpp = 2,3-bis(2-pyridyl)pyrazine, and dpq = 2,3-bis(2-pyridyl)quinoxaline).

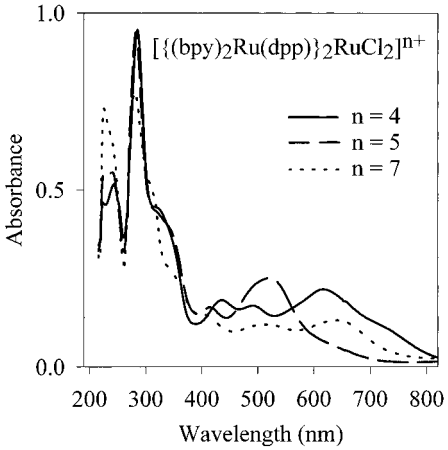

Figure 4. Spectroelectrochemistry of $[\{(bpy)_2Ru(dpp)\}_2RuCl_2]^{4+}$ measured in a 0.1 M Bu_4NPF_6 CH_3CN solution at room temperature (bpy = 2,2′-bipyridine, and dpp = 2,3-bis(2-pyridyl)pyrazine).

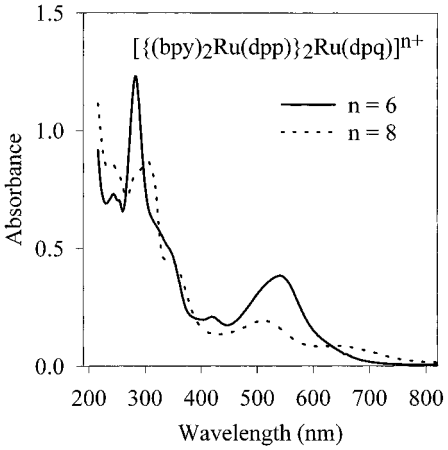

Figure 5. Spectroelectrochemistry of $[\{(bpy)_2Ru(dpp)\}_2Ru(dpq)]^{6+}$ measured in a 0.1 M Bu_4NPF_6 CH_3CN solution at room temperature (bpy = 2,2′-bipyridine, dpp = 2,3-bis(2-pyridyl)pyrazine, and dpq = 2,3-bis(2-pyridyl)quinoxaline).

of these complexes with >90% regeneration of the parent complex. Upon oxidation of a metal center in these types of polyazine-bridged systems, MLCT transitions associated with the metal that has been oxidized are typically shifted out of the visible region of the spectrum.[10a−c,f,11f,15] This can be used to assign the metal involved in a particular MLCT transition. Our group has shown that the oxidation of a $(bpy)_2M(\mu\text{-dpp})$ chromophore leads to a splitting and shifting to lower energy of the band originally at ca. 290 nm in these complexes.[10a,f] This characteristic spectroscopic change can be utilized to assign the nature of the metal oxidation processes in the title trimetallic complexes.

The spectroelectrochemistry of $[\{(bpy)_2Os(dpp)\}_2RuCl_2]^{4+}$ is shown in Figure 2. It was possible to reversibly generate the one- and three-electron oxidized form of this complex. Generation of $[\{(bpy)_2Os^{II}(dpp)\}_2Ru^{III}Cl_2]^{5+}$ gives rise to some very dramatic changes in the visible spectroscopy of this chromophore and small changes in the 290 nm region of the spectrum. The lack of a significant change in the spectroscopy in the 290 nm region indicates the ruthenium nature of this oxidation, as it would be inconsistent with an oxidation of the $(bpy)_2Os(\mu\text{-dpp})$ chromophores.[10a−c,f] Upon ruthenium oxidation, the low-energy peak at 600 nm is lost, consistent with its Ru → dpp CT nature. The tail in the 650−800 nm region is maintained but decreases somewhat in intensity, presumably due to the loss of the overlap from the Ru → dpp CT band. The peak at ca. 750 nm that remains represents the osmium-based ^{3}MLCT. The peak at 512 nm in the synthesized oxidation state is slightly red-shifted and gains some intensity upon generation of the Ru^{III} complex. This is consistent with the Os → dpp CT nature of this transition which experiences a slight red shift upon ruthenium oxidation due to the stabilization of the dpp π^* orbitals. The Os → bpy CT transition at 430 nm is maintained upon ruthenium oxidation, consistent with its assignment. The spectroscopy of the $[\{(bpy)_2Os^{II}(dpp)\}_2Ru^{III}Cl_2]^{5+}$ complex is quite similar to that observed for the $[\{(bpy)_2Os^{II}(dpp)\}_2Ru^{II}(dpq)]^{6+}$ system. This results from the dominance of the two $(bpy)_2Os^{II}(\mu\text{−dpp})$ chromophores on the spectroscopy observed for both complexes. Oxidation of the osmium centers to form the $[\{(bpy)_2Os^{III}(dpp)\}_2Ru^{III}Cl_2]^{7+}$ complex leads to a bleaching of all of the transitions in the visible, consistent with their MLCT nature. The peak at 290 nm shows the characteristic shift and splitting that is indicative of oxidation of the terminal osmium metal centers bound to the bpy ligands.[10a,f]

The spectroelectrochemistry of $[\{(bpy)_2Os(dpp)\}_2Ru(dpq)]^{6+}$ is illustrated in Figure 3. This complex only possesses one oxidative couple within the acetonitrile solvent window. Oxidation of this complex by two electrons to generate $[\{(bpy)_2Os^{III}(dpp)\}_2Ru^{II}(dpq)]^{8+}$ results in some changes in the UV and visible regions of the spectrum. The characteristic shift and splitting of the peak at 290 nm upon metal oxidation is only consistent with an osmium-based redox process.[10a,f] The peaks at 750, 560, and 420 nm are lost upon osmium oxidation, consistent with their osmium-based ^{3}MLCT, ^{1}MLCT, and ^{1}MLCT assignments, respectively. Oxidation of the osmium center with the accompanying loss of the peak at 560 nm reveals the ruthenium-based MLCT bands that occur in this region, i.e., the overlapping Ru → dpp and Ru → dpq CT bands at ca. 520 nm.

The spectroelectrochemistry of $[\{(bpy)_2Ru(dpp)\}_2RuCl_2]^{4+}$ is shown in Figure 4. It was possible to generate the one- and three-electron oxidized form of this complex. Generation of $[\{(bpy)_2Ru^{II}(dpp)\}_2Ru^{III}Cl_2]^{5+}$ gives rise to some very dramatic changes in the visible spectroscopy of this chromophore and no significant changes in the 290 nm region of the spectrum. This establishes the nature of the redox processes as involving the $(\mu\text{-dpp})_2RuCl_2$ metal center.[10a,f] Oxidation of this central ruthenium leads to a loss of the lowest energy MLCT for this complex, the Ru → dpp CT band at 620 nm. The other transitions in the visible remain upon oxidation of the central ruthenium center, consistent with their assignments as being MLCT transitions involving the terminal ruthenium metal

centers. Oxidation of the terminal ruthenium centers to generate $[\{(bpy)_2Ru^{III}(dpp)\}_2Ru^{III}Cl_2]^{7+}$ leads to a splitting and shift of the peak originally at 290 nm, consistent with the oxidation of the terminal $(bpy)_2Ru(\mu-dpp)$ moieties.[10a,f] Oxidation of these terminal ruthenium centers also results in the loss of the peaks at 430 and 496 nm, consistent with their Ru → bpy and terminal Ru → dpp CT nature, respectively. A new peak grows in at 660 nm upon oxidation of the terminal ruthenium centers. An absorbance in this region for $(bpy)_2Ru^{III}(\mu$-dpp) species has been observed by our group in the past and may represent a LMCT (ligand to metal charge transfer) transition to the now partially occupied orbital on the oxidized ruthenium center.[10a]

The spectroelectrochemistry of $[\{(bpy)_2Ru(dpp)\}_2Ru(dpq)]^{6+}$ is illustrated in Figure 5. This complex only possesses one oxidative couple within the acetonitrile solvent window. Oxidation of this complex by two electrons to generate $[\{(bpy)_2Ru^{III}(dpp)\}_2Ru^{II}(dpq)]^{8+}$ results in some changes in the UV and visible regions of the spectrum. The characteristic shift and splitting of the peak at 290 nm upon metal oxidation is only consistent with a terminal ruthenium-based redox process.[10a,f] The peaks at 420 and 540 nm are lost upon terminal ruthenium oxidation, consistent with a terminal Ru → bpy and Ru → dpp CT assignment, respectively. A new peak appears at 660 nm upon generation of the $(bpy)_2Ru^{III}(\mu$-dpp) centers and can be attributed to a new LMCT transition to this metal center.[10a]

It is interesting to note some of the similarities and differences in the spectroelectrochemistry for the osmium- and ruthenium-based $[\{(bpy)_2M(dpp)\}_2RuCl_2]^{4+}$ and $[\{(bpy)_2M(dpp)\}_2Ru(dpq)]^{6+}$ complexes. The $[\{(bpy)_2M(dpp)\}_2Ru(dpq)]^{6+}$ complexes display similar spectroscopy in the synthesized and two-electron oxidized forms. There is a slight red shift in the maxima for the Os systems relative to the Ru systems in the synthesized oxidation state for the overlapping M → dpp, Ru → dpp, and Ru → dpq MLCT transitions at 560 and 540 nm. Oxidation of the terminal metal removes the M → dpp CT component, and then the Os- and Ru-based complexes display similar MLCT energies at ca. 520 nm for the remaining Ru → dpp and Ru → dpq CT transitions. The $[\{(bpy)_2M(dpp)\}_2RuCl_2]^{4+}$ complexes have more varied spectroscopy in the synthesized oxidation state that become similar as the central ruthenium is oxidized. The one-electron oxidized species $[\{(bpy)_2M^{II}(dpp)\}_2Ru^{III}Cl_2]^{5+}$ display similar spectroscopy, with the Os-based system having a red-shifted M → dpp CT band at 540 nm relative to the 520 nm M → dpp CT band for the Ru analog. Both $[\{(bpy)_2M(dpp)\}_2RuCl_2]^{4+}$ complexes display a bleaching of the MLCT transitions throughout the visible and a splitting and shifting of the 290 nm peak upon three-electron oxidation to generate the $[\{(bpy)_2M^{III}(dpp)\}_2Ru^{III}Cl_2]^{7+}$ species. The ruthenium-based complex has a new peak that appears in the 660 nm region upon terminal metal oxidation that is not present in the Os analog, consistent with this peak being a new dpp → Ru LMCT transition.

Conclusions

The terminal dpq complexes, $[\{(bpy)_2M(dpp)\}_2Ru(dpq)]^{6+}$, have been prepared. These new light absorbers display absorbances throughout the UV and visible regions of the spectrum. The all ruthenium complex is emissive at RT, allowing for a convenient probe of the excited state of this complex. These $[\{(bpy)_2M(dpp)\}_2Ru(dpq)]^{6+}$ systems have interesting electrochemistry, with the dpp ligands each reducing by one electron followed by the terminal dpq/dpq$^-$ wave prior to the two μ-dpp$^-$/μ-dpp^{2-} waves due to the stabilized π^* orbitals on the dpq ligand. Synthetic variation of the terminal metal centers and the application of spectroelectrochemistry has been very useful in the understanding of the complex spectroscopy and electrochemistry of these trimetallic complexes. The $[\{(bpy)_2M(dpp)\}_2Ru(dpq)]^{6+}$ systems have very similar spectroscopy, with only minor shifts to lower energy of the Os-based lowest lying M → dpp CT transitions. The $[\{(bpy)_2M(dpp)\}_2RuCl_2]^{4+}$ systems have more varied spectroscopy as a function of the terminal metal, with the osmium systems displaying significantly enhanced absorbance in the 650−800 nm region attributed to ^{3}MLCT transitions. The $[\{(bpy)_2M(dpp)\}_2Ru(dpq)]^{6+}$ systems are a promising new type of supramolecular light absorber that couple two $(bpy)_2M^{II}(\mu$-dpp) chromophores to a central ruthenium metal center that is also coordinated to a dpq bridging ligand. This will allow their incorporation into a wide variety of supramolecular complexes with applications to charge separation and photoinitiated electron collection.[19]

Acknowledgment. We wish to thank the National Science Foundation for their generous support of this research (Grant Nos. CHE-9313642 and CHE-9632713) and Johnson Matthey, an Alfa Aesar Company, for the loan of the ruthenium metal used in this study. Special thanks for Kim Harich for obtaining the FAB-MS data for these complexes.

Supporting Information Available: A figure showing the electronic absorption spectra of $[\{(bpy)_2M(dpp)\}_2RuCl_2\}(PF_6)_4$ (1 page). Ordering information is given on any current masthead.

IC961302Y

(19) Jones, S. W.; Clark, J. A.; Brewer, K. J. work in progress.